Original article
UDC 533.9.07
DOI: https://doi.org/10.18721/JPM.17206

DISCUSSION OF PLASMA FOCUS PARAMETERS AND GAIN/LOSS ENERGY PROCESSES FOR A DESIGNED PLASMA FOCUS DEVICE

A. Nassif [1] ✉, W. Sahyouni [2], O. Zeidan [2]

[1] Al-Wataniya Private University, Hama, Syrian Arab Republic;

[2] Al-Baath University, Homs, Syrian Arab Republic

✉ alaa.nassif.85@hotmail.com

Abstract. In this research, a design for a dense plasma focus device has been developed, the plasma-focus parameters and the processes of gain/loss energy have been studied using the Lee code. The outcome was compared with that for UNU ICTP/PFF dense plasma focus device. The obtained results gave a good agreement between the data on the two devices, they also showed an increase in the linear emission process and thus an increase in the X-ray yield of the designed device compared to UNU ICTP/PFF one.

Keywords: dense plasma focus, Lee code, line emission

For citation: Nassif A., Sahyouni W., Zeidan O., Discussion of plasma focus parameters and gain/loss energy processes for a designed plasma focus device, St. Petersburg State Polytechnical University Journal. Physics and Mathematics. 17 (2) (2024) 71–79. DOI: https://doi.org/10.18721/JPM.17206

Научная статья
УДК 533.9.07
DOI: https://doi.org/10.18721/JPM.17206

ОБСУЖДЕНИЕ ЗНАЧЕНИЙ ПАРАМЕТРОВ ПЛАЗМЕННОГО ФОКУСА И ПРОЦЕССОВ УСИЛЕНИЯ/ПОТЕРИ ЭНЕРГИИ НА МОДЕЛИ УСТРОЙСТВА ФОКУСИРОВАНИЯ ПЛОТНОЙ ПЛАЗМЫ

А. Нассиф [1] ✉, В. Сахьюни [2], О. Зейдан [2]

[1] Частный университет Аль-Ватания, г. Хама, Сирийская Арабская Республика;

[2] Университет Аль-Баас, г. Хомс, Сирийская Арабская Республика

✉ alaa.nassif.85@hotmail.com

Аннотация. Разработана конструкция устройства фокусировки плотной плазмы, и с помощью кода Ли проанализированы параметры как его плазменного фокуса, так и процессов прироста/потерь энергии. Проведено сравнение между полученными результатами и соответствующими данными, относящимися к устройству UNU ICTP/PFF для фокусировки плотной плазмы. В итоге получено хорошее согласие между значениями параметров двух устройств. Установлено увеличение интенсивности линейной эмиссии, а следовательно, увеличение выходной мощности рентгеновского излучения разработанного устройства, по сравнению с таковой для устройства UNU ICTP/PFF.

Ключевые слова: фокус плотной плазмы, код Ли, линейное излучение

Для цитирования: Нассиф А., Сахьюни В., Зейдан О. Обсуждение значений параметров плазменного фокуса и процессов усиления/потери энергии на модели устройства фокусирования плотной плазмы // Научно-технические ведомости СПбГПУ. Физико-математические науки. 2024. Т. 17. № 2. С.71–79. DOI: https://doi.org/10.18721/JPM.17206

Introduction

The phenomenon of dense plasma focus was first discovered by a scientist N. V. Filippov in 1961 [1], then J. W. Mather in 1965 [2], who put two designs for a dense plasma focus device from a geometric point of view (the dimensions of the vacuum chamber) (see Fig. 1). But they are similar in terms of the mechanism of formation and movement of the plasma layer until reaching the focusing stage, and these two designs are also similar in the measurement laws that give the neutron yield and the soft X-ray one. After that, a large number of dense plasma focus devices were manufactured and installed in many laboratories around the world, with operating energies ranging from several joules to megajoules [3].

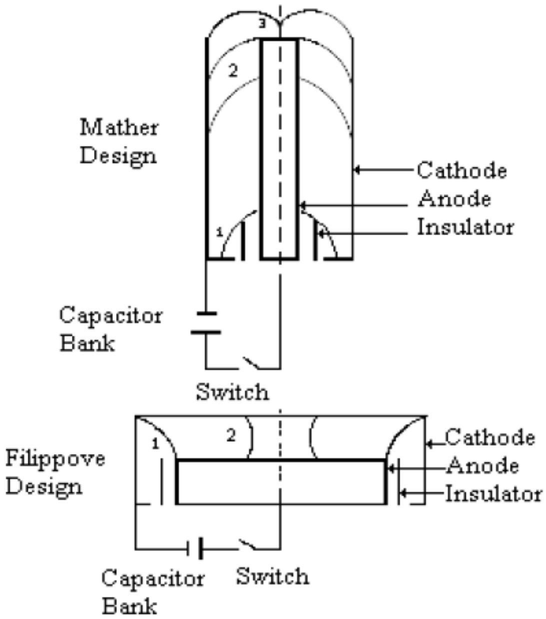

Fig. 1. Schematic sketches showing the geometry of the Mather's (at the top) and the Filippov's (at the bottom) models [3]

A brief description of devices

Soft X-rays are emitted from dense plasma focus by two mechanisms: linear emission and continuous one (recombination and bremsstrahlung) [4 – 6], and hard X-rays also from the collision of electron beams from the collapse of plasma pinch with anode [7 – 9].

As for using deuterium gas, nuclear fusion produces 10^{15} neutrons per second and the emission period is a few tens of nanoseconds making these devices one of the most powerful sources of pulsed radiation in the laboratory [11]. In 2018, W. Sahyouni and A. Nassif studied numerically the emission of soft X-rays from the NX2 plasma focus device using neon gas and found that the maximum value of the soft X-ray yield with the basic parameter of the device Y_{SXR} = 22.6 J at 2.9 Torr, and by shortening the length of the anode and lengthening the radius, the soft X-ray yield increased to 26.01 J with an efficiency of 1.53 % [12]. In 2019, W. Sahyouni and others conducted numerical experiments using the Lee code to study the properties of the ion beam produced by NX2 device when using helium and nitrogen gases with a pressure change, and the results showed that the beam flux was higher with helium, while the ion beam energy was higher with neon because the effective charge of the nitrogen ion being greater and the pinch collapse voltage being higher [13]. In 2021, W. Sahyouni and others conducted a series of numerical experiments to study the effect of the difference in the anode length in NX2 and PF400 devices. The studies showed that the low value of the anode length in the NX2 device affected the axial velocity due to the arrival of a greater amount of energy from the capacitor bank and the highest X-ray value was Y_{SXR} = 4.5 J for the NX2 device and Y_{SXR} = 0.2 J for the PF400 device [14].

Results and discussion

We initially selected the power of the capacitor bank and determined the values of the capacitance, inductance, internal impedance of the electrical circuit, the applied voltage, and the dimensions of the electrodes. Then, these parameters were entered into the Lee model code, and this was to test the quality of these parameters in the plasma focus formation process. After that, the results obtained from the new designed device were compared with those for the UNU ICTP/PFF device for several properties of the plasma focus at two different neon gas pressure values.

Determining electrical circuit parameters. Founding the values of the device's operating power and the parameters of the capacitor bank was mainly based on experimental observations. Therefore, we chose the device's operating energy 3 kJ so that the designed device was in the category of medium-power plasma focus. The capacitance of the capacitor bank was C_0 = 30 μF and the value of inductance L_0 = 110 nH.

Thus, the operating voltage is calculated by the following way:

$$E = \frac{1}{2} C_0 V^2 \Rightarrow V = \sqrt{\frac{2E}{C_0}} = \sqrt{\frac{2 \cdot 3000}{30 \cdot 10^{-6}}} = 14 \text{ kV},$$

and the total discharge current is found by

$$I_0 = \frac{V_0}{\sqrt{\frac{L_0}{C_0}}} = \frac{14000}{0.06} = 321 \text{ kA}.$$

The internal resistance is calculated by

$$r_0 = \frac{1}{4}\sqrt{\frac{L_0}{C_0}} = \frac{1}{4}\sqrt{\frac{110 \cdot 10^{-9}}{30 \cdot 10^{-6}}} = 0.015\Omega.$$

Determination of the dimensions of discharge chamber electrodes. We chose the anode length z = 15 cm, its radius a = 1 cm, and the ratio of the cathode radius to the anode $c = b/a$ = 3.37, so the cathode radius was b = 3.37 cm. Table represents the parameters of the designed device (see the top line).

The designed device was compared with the UNU/ICTP PFF plasma focus device, which had slightly different parameters [12, 14, 15] (see Table, the bottom line).

Table 1

A comparison of parameters of the two devices

E, kJ	C_0, μF	V_0, kV	L_0, nH	I_0, kA	Z_0	a	b	r_0, mΩ
					cm			
The designed device								
3.0	30	14	110	231	15	1.00	3.37	15
UNU/ICTP PFF device								
2.9	30	14	110	231	16	0.95	3.37	15

A comparison of the results on the designed device with the dense plasma focus device UNU/ICTP PFF

Discharge current. The waveform of the total discharge current is considered the most important indicator of the overall performance of plasma focus devices, because it provides energy for all the dynamic, thermodynamic, electrodynamic, and radiation emission processes in the various stages of plasma focus. The waveform of the discharge current contains important information about all the previous processes. On the other hand, the general shape of the discharge current is related to the parameters of the capacitor bank and the dimensions of the discharge chamber electrodes. Therefore, the first step when dealing with plasma focus is to study the discharge current starting from the moment the capacitor bank is closed until the discharge process ends. Therefore, the path of the total discharge current of the designed device was first compared with UNU/ICTP PFF device at the neon gas pressure value 3 Torr.

We notice from Fig. 2 that the maximum value of the discharge current in the designed device is more than its value in the UNU/ICTP PFF device, and that the time required to reach focusing is less. This is due to the difference in the geometric dimensions of the electrodes and the operating energy in the designed device is the highest.

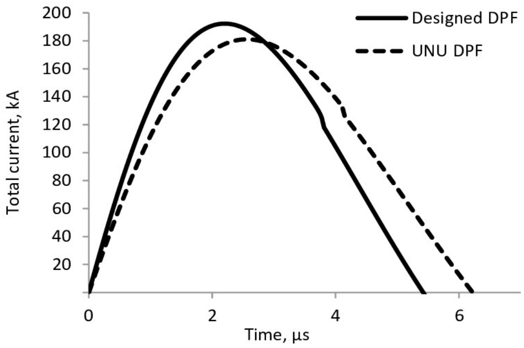

Fig 2. Total discharge current waveforms of the designed device and UNU/ICTP PFF device

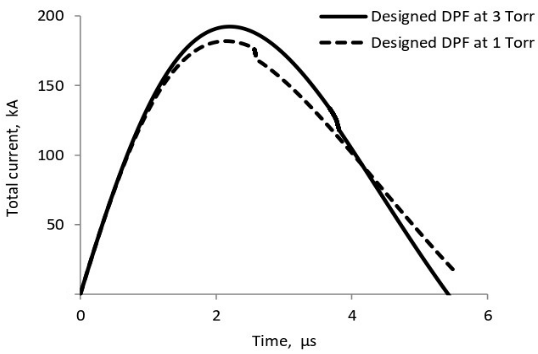

Fig. 3. The total discharge current waveforms of the designed device at pressure values of 1 Torr and 3 Torr

We can also see from Fig. 3 the path of the discharge current for the designed device at the two pressure values of 1 Torr and 3 Torr. We notice the compatibility in the shape of the paths of the two curves and the correspondence between them in the first stage of the discharge process, and they diverge at the peak, noting that the peak decreases in the case of low pressure, in addition to the early end of the discharge process. It is also worth noting that the process of focusing for a pressure of 1 Torr occurs at an instant close to the maximum value of the current, and with a slight reduction in pressure, pinching can occur completely at the peak of the current, and these are ideal conditions for the plasma focus device, in which the device performs as best as possible. Therefore, it can be said that each device, according to its parameters, has ideal experimental conditions that need to be achieved to reach the best X-ray yield.

For example: In the case of pressure 1 Torr, we find that the highest value of the discharge current is 182 kA, and the radial phase begins at 2.55 μs and ends at 2.60 μs. The plasma pinch takes approximately 0.05 ns. As for the pressure value 3 Torr, we find that the highest value of the discharge current is 192 kA, and the radial phase begins at 3.7 μs and ends at 3.8 μs. The plasma pinch takes approximately 0.1 ns, as increasing the value of the gas pressure leads to an increase in the duration of the diagonal phase and the pinch phase.

The vacuum chamber voltage. The changes in the vacuum chamber voltage of the designed device were compared with the one of the UNU/ICTP PFF device (see Fig. 4).

By comparing the two shapes in Fig. 4, we notice the identical shape of the function expressing the vacuum chamber voltage in both devices and the difference in the peak voltage due to the geometric difference between the two devices.

We note in Fig. 5 the changes of the vacuum chamber voltage in terms of the discharge time at the pressure values of 1 Torr and 3 Torr, where the beginning of the peak indicates the end of the axial phase and the beginning of the radial compression phase, which includes within it. The phase of plasma pinch formation where the steep slope of the peak indicates its formation.

It is clear from Fig. 5 that the highest value of the chamber voltage at 3 Torr is 1.62 kV, while at 1 Torr it is 3.30 kV, as the decrease in the value of the neon gas pressure led to an increase in the value of the chamber voltage.

Temperature. Figs. 6 and 7 also show a similarity in the general shape of the two curves, as we notice an exponential increase, then stability in temperature, then a linear decrease with the progression of time, indicating a sharp increase in temperature in the case of low pressure within a shorter time than in the case of high pressure.

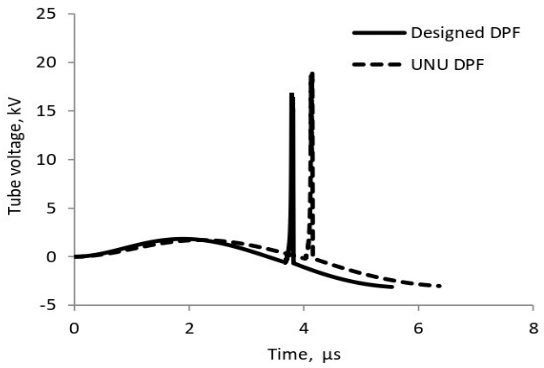

Fig. 4. Time dependences of the vacuum chamber voltage for the designed device and UNU/ICTP PFF one

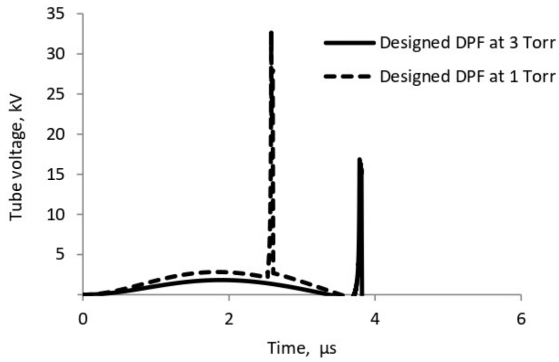

Fig. 5. Time dependences of the vacuum chamber voltage for the designed device at the pressure values of 1 Torr and 3 Torr

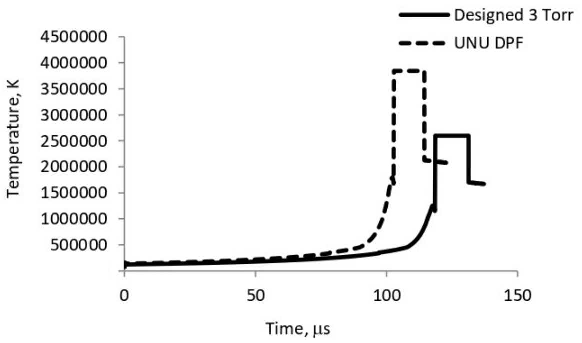

Fig. 6. Time dependences of the plasma temperature for the designed device and the UNU/ICTP PFF one

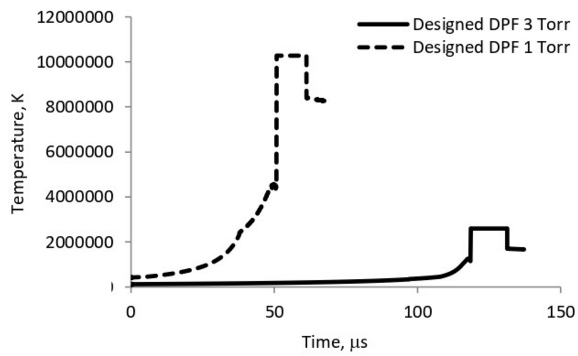

Fig. 7. Time dependences of the plasma temperature for the designed device at the pressure values of 1 Torr and 3 Torr

The stability in temperature in the upper part of the two curves is due to the stability of the speed of the plasma shock wave, and a decrease that occurs after this stability is due to a decrease in the value of the discharge current, that is, the decrease in the value of the energy arriving from the capacitor bank to this stage of the development of the plasma focus.

Energy gain. Joule heating expresses the process that occurs when an electric current passes through a conductor, which leads to the emission of heat. In plasma focus, the Joule heating results from the passage of current through the plasma (transmitter) which leads to an increase in its temperature, and this is what is considered heat gain (energy gain) for the plasma through this process.

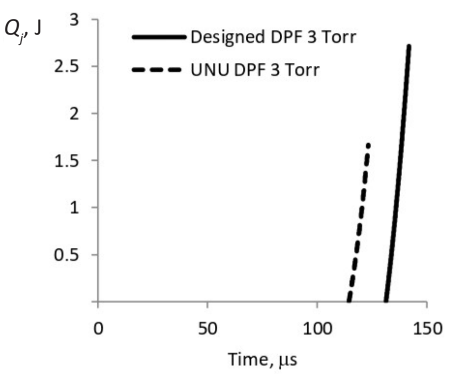

Fig. 8. Joule heating dynamics of the designed and UNU/ICTP PFF devices

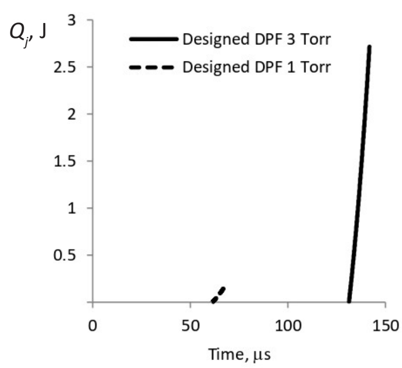

Fig. 9. Joule heating dynamics for the designed device at the pressure values of 1 Torr and 3 Torr

The Joule heating value was compared between the designed device and the (UNU/ICTP) device (Fig. 8) during the radial phase at 3 Torr, where we notice an agreement between the two curves, noting that the designed device acquires higher energy (Joule heating), as the highest value of this energy reaches 2.72 J, while in UNU/ICTP device 1.67 J, due to the difference in geometric dimensions between the two devices.

We also notice from Fig. 9 the value of the Joule heating at 1 Torr and 3 Torr respectively for the designed device, where we can see an increase in the process of energy gain with the increase in the value of the neon gas pressure.

Energy loss. Energy loss in the plasma focus is carried out through three processes: bremsstrahlung → recombination → linear emission.

Bremsstrahlung. Energy is lost by bremsstrahlung as a result of the Coulomb interaction between electrons and ions, which is known as the (free – free) transition of the electron.

By comparing the process of braking energy loss between the designed device and UNU/ICTP one at a single pressure value of 3 Torr, we note that the bremsstrahlung energy loss in the designed device is less than that of the device and this energy loss increases with increasing the neon gas pressure in the designed device (Fig. 10). Fig. 11. represents the bremsstrahlung dynamics for the designed device at the pressure values of 1 Torr and 3 Torr.

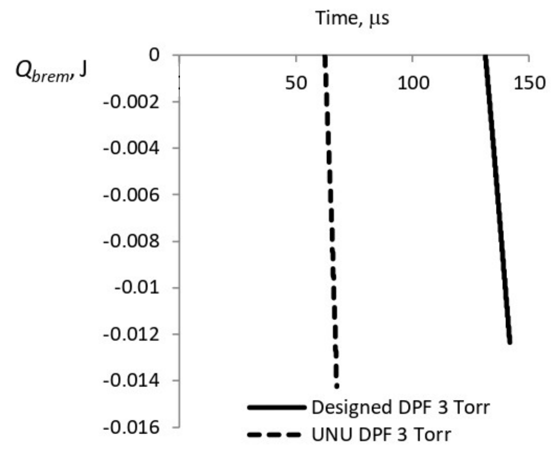

Fig. 10. The bremsstrahlung dynamics of the designed and UNU/ICTP PFF devices

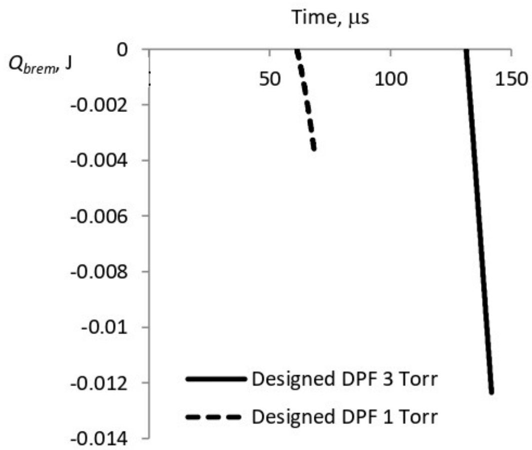

Fig. 11. The bremsstrahlung dynamics for the designed device at the pressure values of 1 Torr and 3 Torr

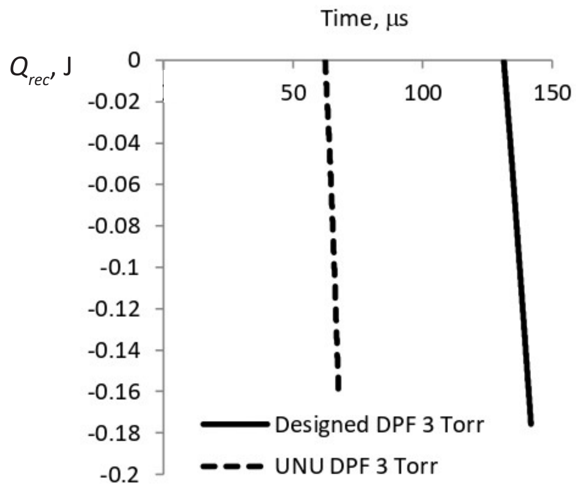

Fig. 12. Recombination dynamics of the designed and UNU/ICTP PFF devices

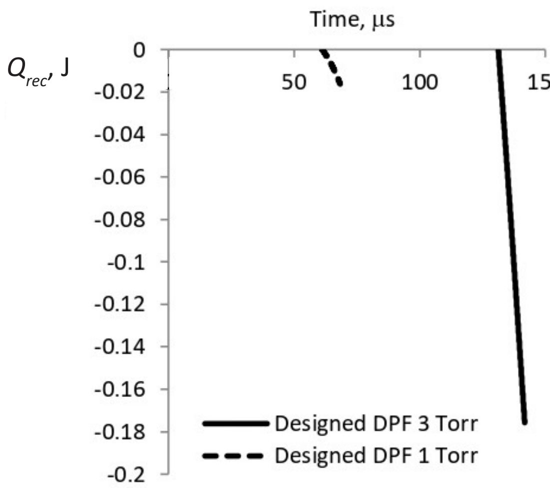

Fig 13. Recombination dynamics for the designed device at the pressure values of 1 Torr and 3 Torr

Recombination. Energy is lost in this process through combining an electron with an ion, or what is known as the (free – bound) transition. It is clear from Figs. 12 and 13 that the designed device loses energy in this process is slightly greater than that for UNU/ICTP device, and also the energy loss increases by recombination in the designed device with an increase in the applied gas pressure.

Line emission. Energy is lost by line emission in the plasma focus through electron transfer to lower ionic states or the so-called (bound – bound) transition.

We notice from Figs. 14 and 15 that the energy loss through line emission in the designed device is slightly higher than that in UNU/ICTP device, and the increase in pressure in the designed device leads to an increase in energy loss through this mechanism.

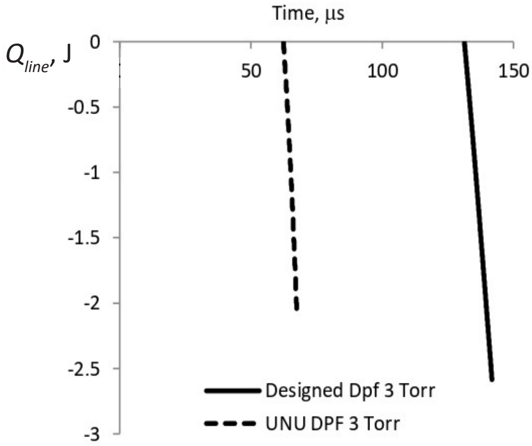

Fig. 14. Line emission dynamics of the designed and UNU/ICTP PFF devices

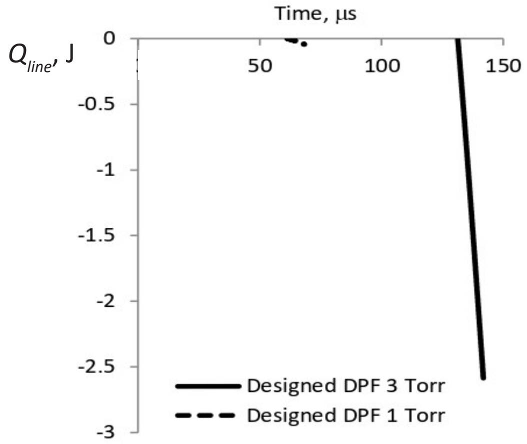

Fig. 15. Line emission dynamics for the designed device at the pressure values of 1 Torr and 3 Torr

Conclusions

The Lee model was used to develop a new design for a plasma focus device working by neon gas, discuss the plasma focus parameters and energy gain/loss processes, and compare their values with those of the UNU/ ICTP PFF device, which was chosen due to the similar operating energy between the two devices and the difference in vacuum chamber dimensions. It was also confirmed that the plasma parameters focus (the voltage, current and temperature) were compatible at two pressure values: of 1 and 3 Torr. The results showed that the designed device gained more energy (by Joule heating), and the energy loss (by bremsstrahlung, recombination, and line emission) was higher. The higher linear emission value in the designed device means that the soft X-ray yield value of the designed device will be greater compared to that of the UNU/ ICTP PFF device.

REFERENCES

1. **Filippov N. V., Filippova T. I., Vinogradov V. P.,** Dense high-temperature plasma in a non-cylindrical Z-pinch compression, Nucl. Fusion, Suppl.; Proc. 1-st Int. Conf. (Salzburg, Austria, 1961). Pt. 2 (1962) 577–587 (in Russian).

2. **Mather J. W.,** Formation of a high-density deuterium plasma focus, Phys. Fluids. 8 (2) (1965) 366–377.

3. **Talebitaher A., Springham S. V., Shutler P. M. E., et al.,** Imaging of plasma focus fusion by proton coded aperture technique, J. Fusion Energy. 31 (3) (2012) 234–241.

4. **Akel M., Lee S.,** Dependence of plasma focus argon soft X-ray yield on storage energy, total and pinch currents, J. Fusion Energy. 31 (2) (2012) 143–150.

5. **Lee S., Saw S. H., Rawat R. S., et al.,** Correlation of measured soft X-ray pulses with modeled dynamics of the plasma focus, IEEE Trans. Plasma Sci. 39 (11-3) (2011) 3196–3202.

6. **Akel M., Al-Hawat Sh., Lee S.,** Numerical experiments on soft X-ray emission optimization of nitrogen plasma in 3 kJ plasma focus SY-1 using modified Lee model, J. Fusion Energy. 28 (4) (2009) 355.

7. **Mahtab M., Taghipour M., Roshani G. H., Habibi M.,** Approach to the highest HXR yield in plasma focus device using adaptive neuro fuzzy inference system to optimize anode configuration, J. Exp. Phys. 2014 (24 June) (2014) 307403.

8. **Di Lorenzo F., Raspa V., Knoblauch P., et al.,** Hard X-ray source for flash radiography based on a 2.5 kJ plasma focus, J. Appl. Phys. 102 (3) (2007) 033304.

9. **Fogliatto E., González J., Barbaglia M., Clausse A.,** A model of hard X-rays emission from free expanding plasma-focus discharges, J. Phys. Conf. Ser. 511 (May) (2014) 012036.

10. **Roomi A., Saion E., Habibi M., et al.,** The effect of applied voltage and operating pressure on emitted X-ray from nitrogen (N_2) gas in APF plasma focus device, J. Fusion Energy. 30 (5) (2011) 413–420.

11. **Syahputra R. F., Farma R., Saktioto, et al.,** Influence of electrical properties on radiation and emission to pinch radius thermal plasma device, J. Phys. Conf. Ser. 1090 (Sept) (2018) 012058.

12. **Sahyouni W., Nassif A.,** Nitrogen soft X-Ray yield optimization from UNU/ICTP PFF plasma focus device, Am. J. Mod. Phys. 8 (6) (2019) 86–89.

13. **Sahyouni W., Nassif A.,** Ion beam properties produced by NX2 plasma focus device with helium and nitrogen gas, Am. J. Mod. Phys. 8 (1) (2019) 1–4.

14. **Sahyouni W., Nassif A., Yousef R.,** Study the effect of anode length on nitrogen plasma pinch dimensions in NX2 and UNU/ICTP PFF dense plasma focus devices, Evol. Mech. Eng. 3 (5) (2021) 000573.

15. **Lee S., Saw S. H.,** Generation of soft X-ray (SXR) from plasma focus, Int. J. Eng. Technol. 1 (1) (2012) 218.

СПИСОК ЛИТЕРАТУРЫ

1. **Филиппов Н. В., Филиппова Т. И., Виноградов В. П.** Плотная высокотемпературная плазма в области нецилиндрической кумуляции *Z*-пинча // Nuclear Fusion. Supplement; Proceedings of the 1st International Conference (Salzburg, Austria, 1961). 1962. Part 2. Pp. 577–587.

2. **Mather J. W.** Formation of a high-density deuterium plasma focus // Physics of Fluids. 1965. Vol. 8. No. 2. Pp. 366–377.

3. **Talebitaher A., Springham S. V., Shutler P. M. E., Lee P., Rawat R. S.** Imaging of plasma focus fusion by proton coded aperture technique // Journal of Fusion Energy. 2012. Vol. 31. No. 3. Pp. 234–241.

4. **Akel M., Lee S.** Dependence of plasma focus argon soft X-ray yield on storage energy, total and pinch currents // Journal of Fusion Energy. 2012. Vol. 31. No. 2. Pp. 143–150.

5. **Lee S., Saw S. H., Rawat R. S., et al.** Correlation of measured soft X-ray pulses with modeled dynamics of the plasma focus // IEEE Transactions on Plasma Science. 2011. Vol. 39. No. 11. Part 3. Pp. 3196–3202.

6. **Akel M., Al-Hawat Sh., Lee S.** Numerical experiments on soft X-ray emission optimization of nitrogen plasma in 3 kJ plasma focus SY-1 using modified Lee model // Journal of Fusion Energy. 2009. Vol. 28. No. 4. P. 355.

7. **Mahtab M., Taghipour M., Roshani G. H., Habibi M.** Approach to the highest HXR yield in plasma focus device using adaptive neuro fuzzy inference system to optimize anode configuration // Journal of Experimental Physics. 2014. Vol. 2014. 24 June. P. 307403.

8. **Di Lorenzo F., Raspa V., Knoblauch P., Lazarte A., Moreno C., Clausse A.** Hard X-ray source for flash radiography based on a 2.5 kJ plasma focus // Journal of Applied Physics. 2007. Vol. 102. No. 3. P. 033304.

9. **Fogliatto E., González J., Barbaglia M., Clausse A.** A model of hard X-rays emission from free expanding plasma-focus discharges // Journal of Physics: Conference Series. 2014. Vol. 511. May. P. 012036.

10. **Roomi A., Saion E., Habibi M., Amrollahi R., Baghdadi R., Etaati G. R., Mahmood W., Iqbal M.** The effect of applied voltage and operating pressure on emitted X-ray from nitrogen (N_2) gas in APF plasma focus device // Journal of Fusion Energy. 2011. Vol. 30. No. 5. Pp. 413–420.

11. **Syahputra R. F., Farma R., Saktioto, Nawi N. D., Rashid N. A., Ismail F. D., Ali J.** Influence of electrical properties on radiation and emission to pinch radius thermal plasma device // Journal of Physics: Conference Series. 2018. Vol. 1090. September. P. 012058.

12. **Sahyouni W., Nassif A.** Nitrogen soft X-Ray yield optimization from UNU/ICTP PFF plasma focus device // American Journal of Modern Physics. 2019. Vol. 8. No. 6. Pp. 86–89.

13. **Sahyouni W., Nassif A.** Ion beam properties produced by NX2 plasma focus device with helium and nitrogen gas // American Journal of Modern Physics. 2019. Vol. 8. No. 1. Pp. 1–4.

14. **Sahyouni W., Nassif A., Yousef R.** Study the effect of anode length on nitrogen plasma pinch dimensions in NX2 and UNU/ICTP PFF dense plasma focus devices // Evolutions in Mechanical Engineering. 2021. Vol. 3. No. 5. October. P. 000573.

15. **Lee S., Saw S. H.** Generation of soft X-ray (SXR) from plasma focus // International Journal of Engineering and Technology. 2012. Vol. 1. No. 1. P. 218.

THE AUTHORS

NASSIF Alaa
Al-Wataniya Private University
International Hama–Homs Highway, Hama, XQ92+PMC, Syrian Arab Republic
alaa.nassif.85@hotmail.com

SAHYOUNI Walid
Al-Baath University
Damascus – Aleppo Highway, Homs, PP75+5VC, Syrian Arab Republic
wsahyouni@albaath-univ.edu.sy

ZEIDAN Ola
Al-Baath University
Damascus – Aleppo Highway, Homs, PP75+5VC, Syrian Arab Republic
ozedan@albaath-univ.edu.sy

СВЕДЕНИЯ ОБ АВТОРАХ

НАССИФ Алаа – *доктор военных наук, профессор инженерного факультета Частного университета Аль-Ватания, г. Хама, Сирийская Арабская Республика.*
XQ92+PMC, Syrian Arab Republic, Hama
alaa.nassif.85@hotmail.com

САХЬЮНИ Валид – *Ph.D., профессор кафедры физики (исследовательский отдел физики плазмы) Университета Аль-Баас, г. Хомс, Сирийская Арабская Республика.*
PP75+5VC, Syrian Arab Republic, Homs, Damascus – Aleppo Highway
wsahyouni@albaath-univ.edu.sy

ЗЕЙДАН Ола – *Ph.D., профессор кафедры физики (исследовательский отдел физики плазмы) Университета Аль-Баас, г. Хомс, Сирийская Арабская Республика.*
PP75+5VC, Syrian Arab Republic, Homs, Damascus – Aleppo Highway
ozedan@albaath-univ.edu.sy

Received 15.07.2023. Approved after reviewing 27.03.2024. Accepted 27.03.2024.

Статья поступила в редакцию 15.07.2023. Одобрена после рецензирования 27.03.2024. Принята 27.03.2024.